

Critical exponent for the viscosity of four binary liquids

Robert F. Berg and Michael R. Moldover

Thermophysics Division, National Bureau of Standards, Gaithersburg, Maryland 20899

(Received 1 April 1988; accepted 8 June 1988)

We have measured the viscosity of four binary mixtures near their consolute points: (1) methanol + cyclohexane, (2) isobutyric acid + water, (3) nitroethane + 3-methylpentane, and (4) 2-butoxyethanol + water. The viscosity data are consistent with the power-law divergence: $\eta \sim |T - T_c|^{-\gamma}$, with an apparent viscosity exponent in the range $0.0404 < \gamma < 0.0444$. Recent theoretical estimates for γ are near 0.032, which is outside the experimental range. The value of γ is independent of whether the critical point is an upper or a lower consolute point and of whether the approach toward T_c is at constant pressure or at constant volume. Our torsion oscillator viscometer is unique in its simultaneous low frequency (~ 1 Hz) and low shear rate (~ 0.1 s $^{-1}$), allowing its use close to the critical point before encountering non-Newtonian fluid behavior associated with critical slowing down. Nevertheless, we find quantitative evidence for viscoelasticity near the critical point.

I. INTRODUCTION

Despite dozens of studies in the last 25 years, the exponent characterizing the weak divergence of the viscosity near fluid critical points has not been accurately determined. This paper will describe new measurements on four very different binary liquids made with a unique viscometer which operates simultaneously at low frequency and low shear rate, thus reducing systematic errors caused by slow fluctuations near the critical point.

We chose the mixtures partly for the varied nature of their noncritical backgrounds, as can be seen by the viscosity data in Fig. 1. In Fig. 2 these same data are drawn on a semilog scale. The resulting similarity of the curves, as well as theory, suggests a multiplicative background. To analyze the data, we assumed that the dependence of viscosity η on reduced temperature t could be described by the function

$$\eta = Ae^{Bt}t^{-\gamma}. \quad (1)$$

The exponent γ characterizes the critical divergence while the parameter B measures the temperature dependence of the noncritical background.

The magnitudes A for the binary liquids varied from 0.003 to 0.02 P. The background parameter B also varied from -8 to $+8$. In addition, by approaching the critical point along a constant volume instead of the usual constant pressure path, for methanol + cyclohexane we were able to change B by a factor of 2.5. In spite of these large variations in background, the viscosity exponent values fall in the range

$$0.0404 < \gamma < 0.0444. \quad (2)$$

This range is narrower than the spread of 13 recent measurements reviewed in Ref. 1, and it excludes the current theoretical prediction² of $\gamma = 0.032$. When reasonable "corrections to scaling" are included in the analysis of the viscosity, the differences in γ between fluids can be accounted for, thus recovering universality. However, such corrections cannot reconcile Eq. (2) with the theoretical value of γ .

Near the critical point, the diverging fluid relaxation

time τ constrains the viscometer's frequency ω and shear rate S . Ideally,

$$\omega\tau \ll 1 \quad \text{and} \quad S\tau \ll 1 \quad (3)$$

if relaxation time effects are to be avoided. There are literally dozens of techniques for measuring viscosity; however, most violate at least one of the conditions of Eq. (3) or are otherwise not suited for measurements near critical points. We therefore constructed a new type of viscometer suited to automated near-critical measurements. This viscometer has the low frequency $\omega/2\pi \approx 1$ Hz and the low shear rate $S \approx 0.1$ s $^{-1}$. We applied it to the critical binary mixtures methanol + cyclohexane (ME + CY), isobutyric acid + water (IBA + H₂O), nitroethane + 3-methylpentane (NE + 3MP), and 2-butoxyethanol + water (2BE + H₂O). The methanol + cyclohexane data, taken along both constant pressure and constant volume paths, have been reanalyzed since an earlier report.³

Despite our efforts, the conditions in Eq. (3) were violated very close to the critical point; thus, we relied on quantitative theories to estimate the effects of shear⁴ and frequency.⁵ Our data provide evidence in support of the predicted frequency effect.

In Sec. II we will give a brief outline of the theoretical context of our measurements and review the standard argument for a multiplicative form of the noncritical background. Section III, on apparatus and technique, will also be brief as we have published a previous description of the viscometer.⁶ Section IV describes the samples and Sec. V describes how we analyzed the data, including effects due to concentration errors, shear, and frequency. Section VI is the conclusion.

II. THEORETICAL EXPECTATIONS

The viscosity η near the critical temperature T_c is characterized by an exponent γ according to

$$\eta \sim t^{-\gamma}, \quad (4)$$

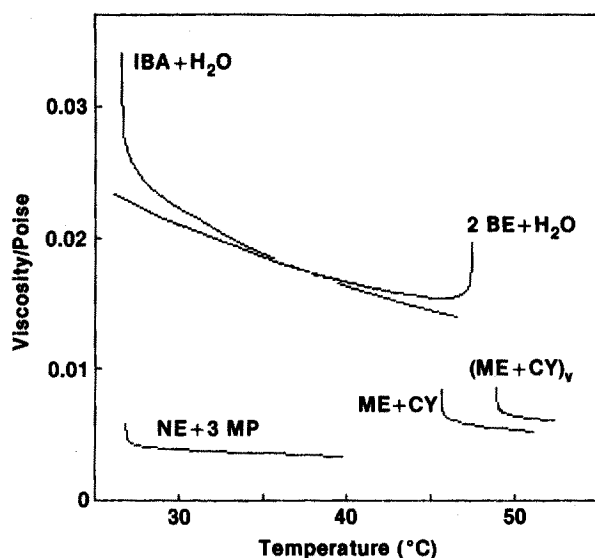


FIG. 1. Measured viscosity vs temperature for four binary mixtures near their consolute points. ME + CY: methanol + cyclohexane, (ME + CY)_v: methanol + cyclohexane at constant volume, IBA + H₂O: isobutyric acid + water, NE + 3MP: nitroethane + 3-methylpentane, 2BE + H₂O: 2-butoxyethanol + water.

where the reduced temperature t is defined by

$$t \equiv |T - T_c|/T_c. \quad (5)$$

Prior to this work, a review¹ of experimental values of y listed 13 values spanning the range $0.032 < y < 0.042$, roughly $\pm 15\%$. This uncertainty contrasts with much more precise knowledge of static exponents. For example, the exponent ν , which describes the divergence of the fluctuation correlation length via

$$\xi = \xi_0 t^{-\nu} \quad (6)$$

is known to within 1%.⁷ (Here ξ_0 is a fluid-dependent amplitude.)

Near critical points, dynamic properties such as thermal conductivity, viscosity, or diffusion are less understood than static properties such as heat capacity because both the theoretical and the experimental studies are more difficult. Universality classes, defined for static properties by the number of spatial dimensions and the tensorial nature of the order parameter, must be further subdivided for dynamical properties according to which conservation laws are pertinent to the system dynamics. Thus a uniaxial ferromagnet and a fluid which belong to the same static universality class might belong to different dynamic universality classes because the dynamics of diffusing spins and particles are quite different.⁸

A key feature of near-critical dynamics is the slow relaxation of fluctuations, which can be characterized by a diverging relaxation time τ . For fluids in three dimensions,

$$\tau \simeq \tau_0 t^{-3\nu - \gamma} \simeq \tau_0 t^{-1.93}. \quad (7)$$

The time τ is that required for a fluctuation region of size ξ to return to equilibrium and is an intrinsic property of the fluid. Typically, the fluid-dependent amplitude τ_0 is such that the time τ is greater than 1 s for achievable reduced temperatures. In contrast, far from T_c , τ is of the order of nanoseconds.

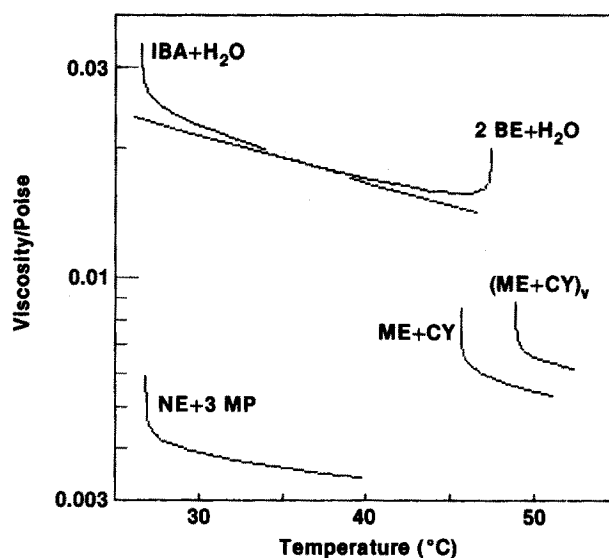


FIG. 2. The data of Fig. 1 redrawn on a logarithmic viscosity scale. The similarity of the curves demonstrates that the divergence of the viscosity is at least roughly proportional to the noncritical viscosity as in Eq. (1).

Although the viscosity diverges near T_c , the experimentally accessible enhancement is small: only 10%–20% in pure fluids such as xenon and 30%–50% in binary fluid mixtures.¹ The dynamic renormalization group theory¹ predicts that the enhancement asymptotically diverges as in Eq. (4) or, in terms of the correlation length,

$$\eta \sim \xi^{x_\eta}, \quad (8)$$

where

$$y = \nu x_\eta. \quad (9)$$

Another approach, mode coupling, employs the idea that nonlinear couplings between relevant hydrodynamic modes (species diffusion and transverse momentum diffusion for a binary liquid) can affect the values of the kinetic coefficients and thus the transport coefficients. Approximately, one has two coupled integral equations⁸ which relate osmotic conductivity and viscosity at wave vector k to each other through the k -dependent osmotic susceptibility $\chi(k)$. Further approximations lead to the prediction of a logarithmically diverging viscosity

$$\eta = \eta_0 [1 + (8/15\pi^2) \ln(Q\xi)], \quad (10)$$

where η_0 is the noncritical fluid viscosity and Q is a fluid-dependent wave vector.

The dynamic renormalization group result of Eq. (8), strictly valid only in the experimentally inaccessible region where $\eta \gg \eta_0$, is inconsistent with Eq. (10). Ohta⁹ pointed out that, if Eq. (10) is viewed as the first term of a power law expansion, consistency can be restored by writing, *ad hoc*,

$$\eta = \eta_0 (Q\xi)^{x_\eta} \quad (11)$$

or, in terms of the reduced temperature t ,

$$\eta = [\eta_0 (Q\xi_0)^{x_\eta}] t^{-\nu x_\eta} \quad (12)$$

$$= [\eta_0 (Q\xi_0)^{x_\eta}] t^{-\gamma}. \quad (13)$$

The quantity in brackets is the divergence amplitude and

includes the fluid-dependent quantities η_0 , Q , and ξ_0 . The form of Eq. (13) is useful because it specifies how to treat the noncritical background viscosity η_0 : the critical divergence is multiplied, not added, to the noncritical background. As early as 1963, multiplicative backgrounds were found useful in describing experimental viscosity data.¹⁰

The numerical value of the viscosity exponent is small: an early prediction⁹ for y , implicit in Eq. (10), was

$$y = (8/15\pi^2)\nu \approx 0.034. \quad (14)$$

We will compare our experimental results to the most recent calculations² which estimate

$$y = \nu x_\eta \approx 0.032 \quad (15)$$

and are claimed to supersede earlier, larger values. See Refs. 1 and 2 for a discussion of the relative merits of these calculations.

For all critical fluids, and especially binary liquids, the temperature dependence of the noncritical viscosity $\eta_0(T)$ cannot be ignored in the analysis of experimental data. One can either attempt an extrapolation of $\eta_0(T)$ from the noncritical region into the critical region or fit the experimental viscosity to a product of a simple analytic function and a divergent term. We have found the latter approach successful in describing our own viscosity data.

In general some sort of "crossover" function which smoothly connects the viscosity behavior near T_c to the noncritical temperature dependence far from T_c ^{1,11,12} should also be considered and we will discuss its use in Sec. V.

Dynamic critical phenomena have been reviewed by Swinney and Henry in 1973,¹³ by Hohenberg and Halperin in 1977,⁷ and by Sengers in 1973¹⁴ and 1985.¹

III. APPARATUS AND TECHNIQUES

Our torsion-oscillator viscometer was explicitly designed for low-frequency, low shear-rate operation near critical points. It has three important accommodations for nearly critical samples. These are precise temperature control (< 1 mK), which is necessary for acquiring data near T_c , low frequency (~ 1 Hz), and small oscillation amplitude, for low shear rates (~ 0.1 s⁻¹). For comparison, capillary viscometers have shear rates from 10 to 1000 s⁻¹. The low frequency and shear rate of our viscometer also ensure that viscous heating of the sample is negligible: of the order of 1 nW. The inertial element of the oscillator (the bob) is hollow and contains the entire sample within a surface of revolution. The elastic element is a quartz fiber which has very low internal friction. The viscosity is obtained from measurements of the decay rate, or decrement, of the torsion oscillations. The viscometer is automated so that several hundred measurements can be made in an overnight run.

Examples of other types of torsion-oscillator viscometers are cited in Ref. 6. These viscometers have either slow periods (< 1 s) but large amplitudes (~ 1 rad) or small amplitudes ($\sim 10^{-6}$ rad) but fast periods (> 100 Hz; see Sec. V B 2: the resulting small penetration depth leads to shear rates of ~ 0.1 s). Our instrument, operating at ~ 1 Hz and $\sim 10^{-3}$ rad amplitude, is significantly superior for critical point measurements. We have published a description⁶ of

this viscometer as equipped with a cylindrical bob; we will therefore be brief in this section.

A. Torsion-oscillator geometries

Our first two binary mixtures were measured with the cylindrical bob and the other two with a newer spherical bob. We initially chose a cylindrical shape because an accurate theory of the viscously damped motion exists¹⁵ and the machining is easier. The internal height and diameter of the cylinder are both 3.8 cm and the thick (0.38 cm) stainless steel shell allows sample pressures up to about 10 MPa.

The newer bob's internal geometry, indicated in Fig. 3, is a 2.5 cm diameter sphere with an upper cylindrical extension 0.54 cm in diameter. The internal volume is about 8 cm³. It was made by soldering two stainless steel hemispheres together; brazing or welding involve greater risk of distortion. The cylindrical extension accommodates thermal expansion of the sample while contributing only a small part to the total decrement. A PTFE disk seals the access hole at the top of the extension.

B. Oscillator motion

The lower surface of the sample-containing bob is a vane which served as a capacitor electrode. It hung close to a second electrode fixed inside the thermostat. Before each

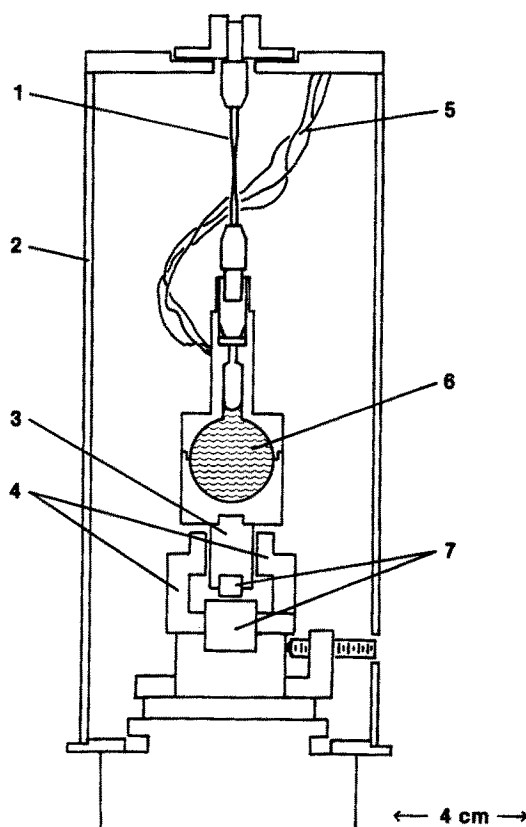


FIG. 3. The spherical torsion oscillator viscometer. Indicated are the (1) quartz torsion fiber, (2) innermost thermostat shell, (3) moving capacitor electrode, (4) stationary electrode, (5) fine wire connections to the oscillator, (6) fluid sample in the spherical bob, and (7) magnetic damper of non-torsional oscillations.

decrement measurement, the torsion oscillations were initiated by a resonant sinusoidal voltage applied between the bob and the fixed electrode. After the excitation ceased, the freely decaying torsion oscillations were characterized by a maximum amplitude θ_0 , a frequency ω , and a decrement D ,

$$\theta(t) = \theta_0 \sin(\omega t) e^{-\omega D t / 2\pi}. \quad (16)$$

Typically, $\theta_0 \approx 1$ mrad and $\omega/2\pi \approx 1$ Hz. To monitor this movement, a commercial capacitance bridge and lock-in amplifier continuously measured the capacitance between the bob's vane and the stationary electrode. The peak voltages of the lock-in output waveform were fitted to the value of the decrement, from which the viscosity was calculated.

C. Thermostat

The thermostat consisted of three nested aluminum shells thermally connected to each other chiefly by radiation. The sample-containing bob was hung inside the innermost shell and acted as a fourth stage of isolation. The bob's thermistor had an absolute accuracy of 0.1 K but was read to a precision of about 0.05 mK by a digital ohmmeter. The temperature difference across the innermost shell was monitored with a thermocouple pile. The temperature of the innermost shell was controlled to ± 0.05 mK using a thermistor read by an ac resistance bridge. The outermost shell, which also acted as the vacuum can for the thermostat, was a 15 cm diameter aluminum cylinder controlled to ± 5 mK.

We avoided excessive temperature differences on the bob during viscosity measurements by turning off the bob heater. The equilibration time of the bob to the inner shell was about 3 h. Exponential temperature sweeps were "programmed" by (1) inducing a temperature difference between the bob and surrounding shell and then (2) allowing the bob temperature to relax to the regulated shell temperature over a period of many hours. During such a sweep, decrement measurements were made and recorded together with the bob's temperatures. Although the sweep rate through T_c ranged from 0.6 to 60 $\mu\text{K/s}$, no dependence of the final results on sweep rate was noted.

IV. SAMPLE CHOICES AND PREPARATION

All four binary liquid mixtures have consolute points with convenient critical temperatures (26 to 49 $^\circ\text{C}$) and have been studied by other groups. In this section we describe the preparation and loading of the mixtures. The critical concentrations Φ_c , will also be given in terms of the weight fraction of the first listed component.

A. Methanol and cyclohexane, ME + CY and (ME + CY),

We chose this mixture to complement light scattering studies close to the critical point. Our methanol + cyclohexane data, first reported in Ref. 3, have been re-analyzed. Other viscosity measurements near the consolute point of this mixture can be found in Ref. 16–19.

The densities of cyclohexane and methanol are matched to within 2%. The hygroscopic methanol can cause problems because water contamination produces a large shift in T_c . We studied this mixture at approximately constant pressure by filling the bob either 1/3 or 2/3 full under nitrogen.

In addition, approximately constant volume measurements [denoted by (ME + CY)_v] were made by completely filling the cylinder with the mixture. To our knowledge, these are the only viscosity measurements at constant volume near a consolute point. The constant volume constraint suppressed thermal expansion and thus reduced the noncritical temperature dependence of the viscosity [B of Eq. (1)] by a factor of 2.5.

For the constant pressure runs, we loaded the cylindrical bob at room temperature from syringes containing the pure components as received from the manufacturers²⁰. For the constant volume runs, we loaded the bob by vacuum distillation as described in Ref. 3.

The compositions of the mixtures were determined by weighing (0.290 methanol by weight). Reported critical compositions for methanol + cyclohexane vary widely. We reviewed the published values using two criteria: (1) the critical temperature and (2) the technique used to determine Φ_c . Studies where T_c differed from our own of 45.6 ± 0.1 $^\circ\text{C}$ by more than 0.5 K were excluded^{21–23} because of this indication of contamination differences.^{21,22} Multiple sample determinations of Φ_c are susceptible to water contamination and typically gave lower Φ_c 's than the other studies. Thus we excluded these also.^{24–26} The remaining studies^{18,27–29} were bracketed by the values $\Phi_c = 0.292 \pm 0.003$ (methanol weight fraction).

B. Isobutyric acid and water, IBA + H₂O

This mixture also has pure components well matched in density but, unlike ME + CY, is not sensitive to water contamination. Examples of earlier critical viscosity measurements near the consolute point can be found in Refs. 30–32.

We loaded the cylindrical bob in air with distilled water and with purified isobutyric acid provided by Greer at the University of Maryland. Several compositions near Φ_c were used. The results reported here are for $\Phi = 0.396$ (weight fraction of the provided isobutyric acid fluid, which includes a small amount of water). To determine the critical concentration, a study was made of the height of the liquid–liquid meniscus in a series of samples near Φ_c . We found $\Phi_c = 0.394 \pm 0.002$.

C. Nitroethane and 3-methylpentane, NE + 3MP

This mixture has been studied several times by capillary viscometry. Values of y in the range $0.035 < y < 0.039$ have been reported.^{1,33–36} Also, y has been roughly estimated from a light scattering study.³⁷ The fluctuation relaxation time is the fastest of the four mixtures, reducing the importance of shear and frequency effects near T_c .

The mixture components³⁸ were obtained from Sengers' group at the University Maryland. They were loaded at room temperature, under nitrogen, into the spherical bob at $\Phi = 0.465$ weight fraction nitroethane (0.500 mole fraction). This concentration is close $\Phi_c = 0.461 \pm 0.001$ (0.495 mole fraction) which we obtained by replotting the original density data of Wims and McIntyre³⁹ as a function of t^β and converting the resulting ρ_c to the corresponding critical mole and weight fractions using density⁴⁰ and volume of mixing⁴¹ data. We note that $\Phi_c = 0.500$ is often

quoted for this mixture; however, Burstyn and Sengers³⁷ mention a comparable discrepancy.

D. 2-Butoxyethanol and water, 2BE + H₂O

This last mixture is interesting because it has an easily accessible lower consolute point. Several groups have studied the critical viscosity.^{42,43} In comparison with NE + 3MP, water contamination is not a problem, but the fluctuation relaxation time amplitude t_0 is 50 times slower. Thus, frequency and shear-dependent effects were seen far from T_c .

We loaded distilled water and commercially available 2-butoxyethanol⁴⁴ into the spherical bob at 0.299 weight fraction 2-butoxyethanol. Because literature values for Φ_c vary, we used a meniscus location study to obtain the critical weight fraction: $\Phi_c = 0.300 \pm 0.002$.

V. DATA SELECTION AND FITTING

In this section we will first describe how we converted decrements to viscosities. Then we will discuss the effects of nonzero shear, frequency, and concentration error close to the critical point and the consequent limits placed on the viscosity data. The final portion deals with the methods used to fit our data, with emphasis placed on the multiplicative background.

All the data, in averaged or original form on diskette, are available from the authors upon request.⁶⁰

A. Decrement to viscosity conversion: $D \rightarrow \eta$

Roughly 1% of the several thousand decrement measurements were rejected because the exponential fit to the oscillator motion [see Eq. (16)] had large errors caused by mechanical disturbances of the viscometer. The remaining decrement data were converted to viscosities as described below.

1. Cylinder

The background decrement, that part of the decrement not due to the sample viscosity, was first accounted for. It resulted from the bending of wires attached to the bob, the viscosity of residual gas in the thermostat, and, for the partially filled cylinder, the vapor's viscosity. The first two contributions were measured with the bob entirely empty. The third contribution was estimated from knowledge of the sample's vapor pressure and viscosity.

After subtracting the background decrement, several other minor corrections were needed. For the cylinder, the most important of these were due to the meniscus curvature caused by wetting. These corrections are discussed in Ref. 6.

Finally, the theory derived by Newell and co-workers¹⁵ was used to convert the measured decrements to viscosities. This was conveniently done using a cubic "working equation"⁴⁵ accurate to 0.1%. This theory requires, as input parameters, the sample mass, sample density, bob moment of inertia and internal dimensions, oscillator period, and background decrement.

As a check on the accuracy of the cylindrical viscometer, we measured the viscosity of water over the range of

30 to 60 °C. Because water may not perfectly wet the bob's walls the meniscus correction had one free parameter: the contact angle. By setting this angle to zero, data sets with the bob 1/3 and 2/3 full agreed with each other within the scatter of the data ($\pm 0.4\%$) and also agreed with the accepted temperature dependent viscosity of water⁴⁶ within 1%.

2. Sphere

Decrement data from the spherical bob were reduced by solving an equation of motion derived by Kearsley [Eq. (10) in Ref. 47]. Because this involves finding the zeros of a non-analytic complex function, we used Newton's method for the case of a double-valued function of two variables. Unlike the cylindrical bob, meniscus corrections were not needed (see Fig. 3). A small correction for fluid contained in the cylindrical extension was estimated by assuming that the viscous penetration depth was small compared to the radius of the extension.

Measurements on water were made between 20 and 65 °C, a range over which its viscosity changes by a factor of 2. The results were uniformly in error by about 5% of which roughly half could be traced to a slight asphericity of the bob. We therefore calibrated the spherical viscometer with water to an accuracy of $\pm 0.5\%$ by reducing subsequent decrement data with a 0.9% larger effective sphere radius.

B. Limits on data close to T_c

1. Concentration

Measurements close to the critical point of a binary liquid imply accurate control of concentration as well as temperature. All of our samples were prepared at nominal critical concentrations based on a single reported value for each mixture. We determined the actual critical concentrations Φ_c as described in Sec. II.

In the following paragraph we will show how, if the concentration difference from critical is known, the deviation of viscosity from its value on the critical isopleth can be estimated using a parametric equation of state valid near the critical point. The restricted cubic model⁴⁸ relates the reduced temperature t and the order parameter Φ to the parameters r and θ :

$$t = r(1 - b^2\theta^2), \quad (17)$$

$$\Delta\Phi \equiv \Phi - \Phi_c = kr^\beta\theta(1 + c\theta), \quad (18)$$

where $b^2 \simeq 1.2766$ and $c \simeq 0.055$ are universal constants. The fluid-dependent constant k is proportional to the amplitude B_Φ of the coexistence curve:

$$k = \frac{(b^2 - 1)^\beta}{(1 + c)} B_\Phi, \quad (19)$$

where

$$\Phi - \Phi_c = \pm B_\Phi t^\beta \quad (20)$$

gives the shape of the coexistence curve. The correlation length ξ varies as

$$\xi = \xi_0 r^{-\nu} R(\theta) \simeq \xi_0 r^{-\nu} (1 + 0.16 \theta^2). \quad (21)$$

Thus, the deviation of ξ on a noncritical isopleth is

$$\frac{\Delta\xi}{\xi} \equiv \frac{\xi(t,0) - \xi(t,\Delta\Phi)}{\xi(t,0)} = (\nu b^2 - 0.16) \left[\frac{\Delta\Phi}{kt^\beta} \right]^2. \quad (22)$$

Using Eq. (8), the corresponding deviation of the viscosity is then

$$\frac{\Delta\eta}{\eta} = x_\eta \frac{\Delta\xi}{\xi} = x_\eta (\nu b^2 - 0.16) \left[\frac{\Delta\Phi}{kt^\beta} \right]^2. \quad (23)$$

Equation (23) can be solved for the reduced temperature t which corresponds to a given viscosity deviation $\Delta\eta/\eta$. Using Eqs. (19) and (20) in Eq. (23), this temperature is

$$t = \frac{\{[x_\eta(\nu b^2 - 0.16)]^{1/2}(1+c)\}^{1/\beta} \left[\frac{\Delta\Phi}{B_\Phi(\Delta\eta/\eta)^{1/2}} \right]^{1/\beta}}{(b^2 - 1)} \quad (24)$$

or

$$t \approx 0.024 \left[\frac{\Delta\Phi}{B_\Phi(\Delta\eta/\eta)^{1/2}} \right]^{1/\beta}. \quad (25)$$

Table I lists the reduced temperatures at which the estimated concentration error for the four binary liquids leads to a relative viscosity error of 0.5% ($\Delta\eta/\eta \approx 0.005$). The quantities $\Delta\Phi$ and B_Φ in Eq. (25) were converted to weight fraction "units" where necessary.

2. Shear

Near T_c , shear can reduce the observed viscosity ("shear thinning")^{5,49} and shift the critical temperature.^{50,51} Here, we show that our shear rates are sufficiently small to avoid these concerns.

First, the relevant relaxation time τ for each fluid mixture must be estimated from the correlation length ξ and diffusion coefficient D^* ^{1,7,52}:

$$\tau = \frac{\xi^2}{D^*} \approx \frac{6\pi\xi^3\eta}{1.03k_B T} \approx \frac{6\pi\xi_0^3\eta_0}{1.03k_B T_c} t^{-(3\nu+y)} \equiv \tau_0 t^{-(3\nu+y)}. \quad (26)$$

Table II summarizes the fluctuation relaxation amplitudes τ_0 for these mixtures.

Next, the fluctuation time is compared with the maximum shear rate in the viscometer,

$$S = \frac{R\omega\theta_0}{\delta} \quad (27)$$

which we calculated from the oscillator radius R , frequency ω , and maximum amplitude θ_0 . The viscous penetration length δ depends on the fluid viscosity η and density ρ :

TABLE II. Relaxation time amplitude $\tau_0 \equiv (6\pi\eta_0\xi_0^3)/(1.03k_B T_c)$.

Mixture	η_0/P	ξ_0/nm	T_c/K	$\tau_0/10^{-11} \text{ s}$
ME + CY	0.0048	0.324 (Refs. 23 and 58)	318.8	6.8
IBA + H ₂ O	0.0200	0.362 (Ref. 59)	299.8	42
NE + 3MP	0.0033	0.216 (Ref. 52)	300.0	1.5
2BE + H ₂ O	0.0117	0.524 (Ref. 43)	320.5	69

$$\delta = \sqrt{\frac{2\eta}{\rho\omega}}. \quad (28)$$

Oxtoby⁵ measures shear effects through the dimensionless parameter

$$\lambda \equiv \frac{S\tau}{6\pi}. \quad (29)$$

A small extrapolation of his Fig. 1 indicates a 0.5% effect in the viscosity at $\lambda \approx 0.13$. The corresponding reduced temperature is

$$t = \left[\frac{S\tau_0}{6\pi\lambda} \right]^{1/1.93}. \quad (30)$$

Using Eq. (30), we list in Table III the reduced temperatures where a 0.5% effect in the viscosity is expected. As with the effect of concentration error, shear thinning is not important for any of the four fluids above $t = 4 \times 10^{-6}$. (The frequency effect is mentioned in the following section.)

The other expected effect of shear is a small shift ΔT_c of the critical temperature^{50,51} which we ignore. The normalized shift

$$\frac{\Delta T_c}{T_c} = -\nu(\tau_0 S)^{1/1.93} \quad (31)$$

is proportional to a coefficient ν which has been measured for our most viscous mixture: isobutyric acid + water.⁵¹ The measured value $\nu = 0.019$ yields the negligible result $\Delta T_c/T_c = 6 \times 10^{-8}$. The T_c shift for the other mixtures should be comparably small.

3. Frequency

In spite of always operating below 2 Hz, we observed frequency effects near T_c . We accounted for these effects by using the theory of Bhattacharjee and Ferrell.⁴ A recent review⁵³ is useful for understanding these papers.

Frequency effects can be interpreted as viscoelasticity, or a complex viscosity:

$$\eta(\omega\tau) \equiv \eta_1(\omega\tau) + i\eta_2(\omega\tau). \quad (32)$$

TABLE I. Reduced temperature where a 0.5% effect due to concentration error is predicted by Eq. (25). Concentration error $\Delta\Phi$ and coexistence curve amplitude B_Φ are in terms of weight fraction.

Mixture	$\Delta\Phi$	B_Φ	$t(\text{conc.})$
ME + CY	-0.002 ± 0.003	0.75 (Ref. 28)	1×10^{-6}
IBA + H ₂ O	+0.002 ± 0.002	0.54 (Refs. 56 and 57)	3×10^{-6}
NE + 3MP	+0.004 ± 0.001	0.97 (Ref. 39)	4×10^{-6}
2BE + H ₂ O	-0.001 ± 0.002	0.68 (Ref. 43)	2×10^{-7}

TABLE III. Reduced temperatures where 0.5% effects in the critical viscosity due to shear [Eq. (30)] and frequency [Eq. (33)] are expected. Viscoelasticity enhances the viscosity at $\omega\tau \approx 5$.

Mixture	Shear/s ⁻¹	$t(\text{shear})$	$(\omega/2\pi)/\text{Hz}$	$t(\omega\tau \approx 5)$
ME + CY	0.09	1×10^{-6}	0.60	5×10^{-6}
IBA + H ₂ O	0.05	2×10^{-6}	0.53–0.59	12×10^{-6}
NE + 3MP	0.29	1×10^{-6}	1.47	4×10^{-6}
2BE + H ₂ O	0.16	4×10^{-6}	1.47	25×10^{-6}

Both η_1 and η_2 are universal functions of the product $\omega\tau$ of the oscillator frequency and the relaxation fluctuation time. As Fig. 4 indicates, η_2/η_1 is small. To first order,⁴ the viscometer measures an effective viscosity which is real:

$$\eta_e(\omega\tau) = \eta_1 + \eta_2 \equiv F(\omega\tau)\eta(\omega\tau=0). \quad (33)$$

The real function $F(\omega\tau)$ is the ratio between $\eta_e(\omega\tau)$ and the zero-frequency viscosity $\eta(0)$. [Note that Bhattacharjee and Ferrell use the convention $\exp(-i\omega t)$; using $\exp(+i\omega t)$ makes η_2 a negative function and then the effective viscosity given by $\eta_1 - \eta_2$.]

Naturally, $F(\omega\tau)$ approaches unity far from T_c . Surprisingly though, $F(\omega\tau)$ is not monotonic. Figure 4 shows that $F(\omega\tau) > 1$ near $\omega\tau \approx 5$. This enhancement of the effective viscosity has not been mentioned before. Table III lists the reduced temperatures where $\omega\tau \approx 5$ for the binary mixtures. We explicitly included $F(\omega\tau)$ in the fitting function. This is justified by the insensitivity of $F(\omega\tau)$ to errors in the relaxation time amplitude τ_0 and by the small size ($\sim 0.5\%$) of the resulting corrections in the experimental range of temperatures.

C. Range of reduced temperatures

As explained above, effects due to concentration error and nonzero shear cut off the viscosity divergence close to T_c . Therefore we fit no data at reduced temperatures below $t = 10^{-5}$ (3 mK from T_c). This conservative cutoff is a factor of 2 to 10 larger than the shear and concentration bounds listed in Tables I and III.

Far from T_c the viscosity temperature dependence is dominated by noncritical behavior. We did not fit the data at reduced temperatures larger than $t = 10^{-1.7}$ (6 K from T_c). Our motivation for this is as follows:

One approach to determining the "background" viscos-

ity is to extrapolate into the critical region a function fitted to viscosity data "far" from T_c . Unfortunately, even 20 K away from T_c the critical enhancement may be as much as a 10% effect. Also, the form of the background temperature dependence is not well known. For example, the Arrhenius function, adequate for some liquids, fails for associated liquids such as water. To avoid these problems we simply restricted the range of reduced temperatures, characterized the background by an exponential function,

$$\eta(\text{noncritical}) \sim Ae^{Bt} \quad (34)$$

and fitted the parameters A and B . The differences between Eq. (34) and another representation such as the Arrhenius or Vogel-Fulcher form are negligible below $t = 10^{-1.7}$.

D. Fitting equations

1. Averaged data

The viscosity data sets were handled in logarithmic form, averaged in bins 0.1 decade wide in t . Figure 5 gives an example of an averaged data set.

The nonlinear fits minimized the sums of square deviations of the averaged logarithmic data from the fitting function over the reduced temperature range

$$10^{-1.7} > t > 10^{-5.0}. \quad (35)$$

Each data point was given equal weight. Estimates of the error in the viscosity exponent γ (see Fig. 7) were made by allowing the other fit parameters to freely vary, thus accounting for possible correlations with the errors of other parameters.

2. Multiplicative background with frequency correction

To describe our viscosity data, we multiplied Eq. (1) by the function $F(\omega\tau)$ of Eq. (33) to incorporate nonzero frequency effects:

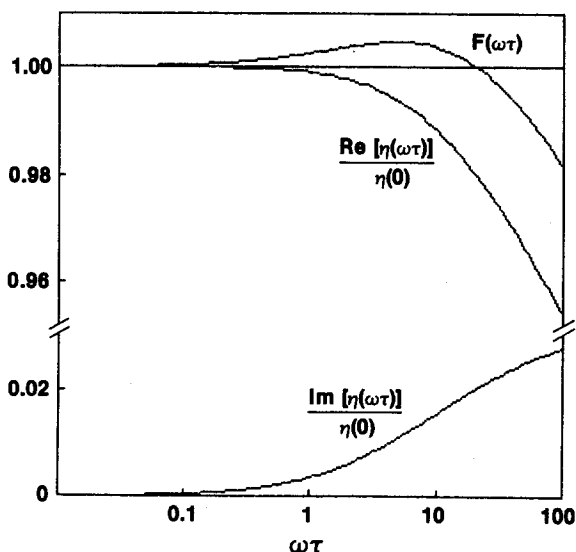


FIG. 4. The frequency effects of Eqs. (32) and (33). The real and imaginary components of the viscosity as fractions of the zero-frequency viscosity $\eta(0)$. Their sum $F(\omega\tau)$ is unity far from T_c and increases by $\sim 0.5\%$ at $\omega\tau \approx 5$ before monotonically falling toward zero. These functions were computed numerically from Eqs. (2.4), (2.13), (3.16), (3.17) and (5.1)–(5.4) of Ref. 4.

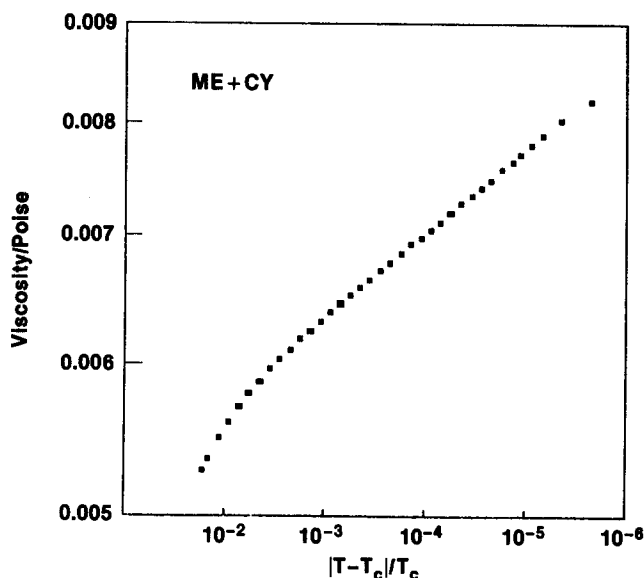


FIG. 5. Averaged viscosity data for the methanol + cyclohexane mixture. The slope of the curve at small reduced temperatures is the viscosity exponent γ .

$$\eta = Ae^{Bt} t^{-\gamma} F(\omega\tau) \quad (36)$$

Equation (36) absorbs both the background magnitude at T_c and the product $(Q\xi_0)^{\gamma}$ into the single parameter A [the factor in brackets in Eq. (13)]. The function $F(\omega\tau)$ has no free parameter. Its argument was converted to reduced temperature using the experimental frequencies and the relaxation time amplitudes listed in Tables II and III.

We allowed the critical temperature T_c to be a fourth, free parameter by modifying Eq. (36) as follows:

$$\log(\eta) = \log(A) - \gamma \log(t + \Delta t) + B(t + \Delta t) + \log[F(t + \Delta t)], \quad (37)$$

where Δt is essentially equivalent to a shift in T_c of

$$\Delta T_c/T_c = \Delta t. \quad (38)$$

We expected the maximum decrement to occur at T_c within the precision allowed by the temperature interval between successive decrement measurements (0.2 to 2 mK). For all but one of our 17 runs, this was true: the T_c defined by the maximum decrement and the T_c found by fitting the viscosity data agreed.

Equation (37), with the four free parameters of A , B , γ , and Δt , describes our viscosity data very well as the deviations plotted in Fig. 6 show. Table IV lists the parameters associated with Fig. 6.

The number of free parameters can be reduced from 4 to

TABLE IV. Typical fit parameters for Eq. (37) for $10^{-1.7} > t > 10^{-5.0}$. A = noncritical amplitude, B = noncritical temperature dependence, $\Delta t = \Delta T_c/T_c$ = shift in fitted T_c from temperature of largest viscosity point, γ = viscosity exponent; critical viscosity $\eta \sim t^{-\gamma}$.

Mixture	A/P	B	Δt	γ
ME + CY	0.004 82	- 4.43	- 1.56×10^{-6}	0.0410
(ME + CY) _v	0.005 18	- 1.67	+ 0.30×10^{-6}	0.0404
IBA + H ₂ O	0.020 04	- 7.90	+ 0.15×10^{-6}	0.0436
NE + 3MP	0.003 31	- 2.50	+ 0.78×10^{-6}	0.0419
2BE + H ₂ O	0.011 94	+ 7.79	- 1.51×10^{-6}	0.0419

3 by requiring $\Delta t = 0$. The fitted range of reduced temperatures must then be restricted to reflect the uncertainty in T_c as determined by the largest decrement; as a result the values for the three free parameters are essentially unchanged.

3. Crossover effects

Although Eq. (37) adequately describes our viscosity data, the resulting values of γ for the four fluid mixtures disagree strongly with current theory and somewhat with each other (see Table IV and Fig. 7). Because these data were not taken in the asymptotic regime, we investigated how crossover modifications of Eq. (37) could affect the exponent γ of the two fluids with extreme values of γ : ME + CY (nominally $\gamma \approx 0.041$) and IBA + H₂O ($\gamma \approx 0.044$). We found that agreement between these fluids could be obtained, but that agreement with the theoretical value $\gamma = 0.032$ was not possible over the full range $10^{-1.7} > t > 10^{-5.0}$.

First we tried using crossover forms proposed by Bhattacharjee *et al.*¹¹ for their limiting cases of $q_D/q_C = 0$ and $q_D/q_C = \infty$. Agreement between ME + CY and IBA + H₂O could be obtained only for the latter case and only by increasing γ . For ME + CY run, γ was increased from 0.041 to 0.044 but the cost was a significant increase in χ^2 (goodness of fit) and implausible positive deviations in the region $10^{-5} > t > 10^{-6}$.

We also used a more general "correction-to-scaling" approach of multiplying Eq. (36) by the factor $(1 + at^\Delta)^x$. If Wegner corrections to ξ are the most important corrections to the viscosity, then $\Delta \equiv 0.5$ and, according to Eq. (8), $x = x_\eta$. Then the universality of the exponent γ can be preserved, e.g., by choosing $a \equiv +3$ for ME + CY and $a \equiv 0$ for IBA + H₂O. Using $\Delta \equiv \nu = 0.63$, as suggested by Olchowy and Sengers,⁵⁴ gave similar results. Although universality can be preserved, agreement with the theoretical value of γ could not be forced over the 3.3 decade range $10^{-1.7} > t > 10^{-5.0}$ with any Δ in the range for $0 < \Delta < 1$.

We also investigated the behavior of the same correction-to-scaling function when restricted to only 2 decades in t ($1^{-3.5} > t > 10^{-5.5}$). For $x = x_\eta$, the theoretical value $\gamma = 0.032$ was consistent with the data, within the experimental resolution of $\pm 0.2\%$, only for $\Delta < 0.01$. For $x = 1$, $\Delta < 0.2$ was necessary. We concluded that a single correc-

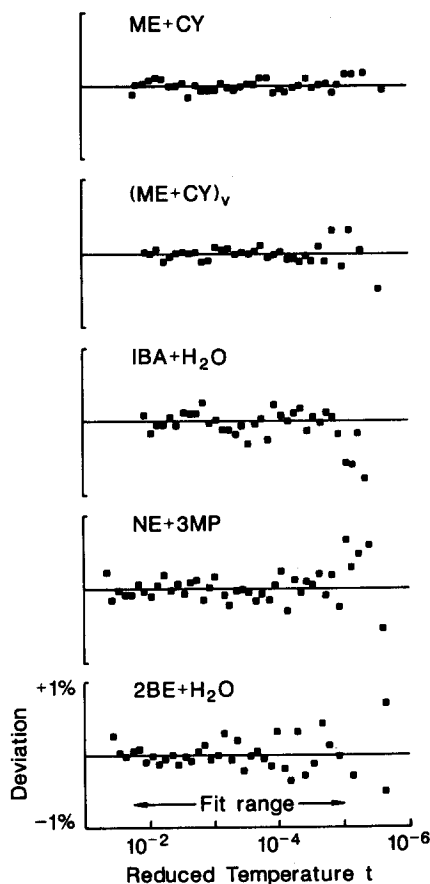


FIG. 6. Deviations from Eq. (37) for five runs using the parameters listed in Table IV.

tion-to-scaling term can reconcile the experimental and theoretical viscosity exponents only over two decades of reduced temperature and then only with surprisingly small values of the correction exponent Δ .

4. Background effects

Figure 7, intended to show the independence of y from the background, nevertheless suggests a correlation between y and the background parameter B . We considered several possible changes to the background functional form, namely the term Bt of Eq. (37). Using an Arrhenius form B/T or adding a second-order term Ct^2 had a negligible effect on y . However, inclusion of an additive background η_1 to Eq. (1) is difficult to distinguish from a change in y , as was pointed out by Calmettes.⁵⁵ Modification of Eq. (1) to

$$\eta = Ae^{Bt} t^{-y} + \eta_1 \quad (39)$$

is approximately equivalent to

$$\eta = A' e^{Bt} t^{-y'}, \quad y' \equiv y(1 - \eta_1/A). \quad (40)$$

Without increasing χ^2 more than 5%, the ratio η_1/A' could be varied as much as ± 0.1 , leading to corresponding shifts in y of ± 0.003 . This was enough to accommodate a universal value of y through appropriate choices of η_1 for the various fluids, but it was insufficient to reduce y to the theoretical value.

5. Other possibilities

Fits using Eq. (37) over the more restricted ranges

$$10^{-1.7} > t > 10^{-4} \quad \text{and} \quad 10^{-3} > t > 10^{-5} \quad (41)$$

did not significantly change the values of y . Fits attempted using the simple mode-coupling form of Eq. (10) were unsuccessful and gave large systematic deviations.

We considered the effect of an error D_1 in the estimate of

the background decrement, the small part of the total decrement D not due to the sample (see Sec. V A). In the thin penetration depth limit, and for D_1 small compared to D , the viscosity exponent y would be shifted to an apparent value of

$$y' = y(1 + D_1/D). \quad (42)$$

For the fluids measured in the cylinder (ME + CY and IBA + H₂O), a 100% error in the background decrement leads to $D_1/D < 0.01$. The corresponding limit for the fluids measured in the sphere (NE + 3MP and 2BE + 3MP) is $D_1/D < 0.05$. Thus, plausible errors in the background decrement are insufficient to explain the observed differences in y between fluids.

As a check on other possible systematic errors, we compared our viscosity measurements at $t = 10^{-2}$ to the results of other groups. Although the results in Table V were not corrected for differing critical temperatures or concentrations, most show agreement to within 3%.

VI. CONCLUSIONS

A. Multiplicative hypothesis

The multiplicative hypothesis works extremely well for the four binary mixtures. Despite widely different background viscosities, systematic deviations from Eq. (37) are typically less than 0.2% over more than 3 decades in reduced temperature.

B. Viscosity exponent

Fits to Eq. (37) yield exponent values in the range

$$0.0404 < y < 0.0444. \quad (43)$$

This definitely disagrees with current predictions.² As shown in Fig. 7, there are small differences among the four fluids.

Two questions can be asked about the experimental exponents. First, are they consistent with universality? Second, are they consistent with theoretical predictions? If Eq. (36) is the true functional form then the respective answers are "maybe" and "no". However, because the viscosity measurements were not made in the truly asymptotic regime where $\eta \gg \eta(\text{background})$ it is possible that important corrections to Eq. (36) are needed. Two candidates for such corrections are crossover effects (Sec. V D 3) and an additive component of the background (Sec. V D 4). We found neither correction was able to reconcile our data with the theoretical value $y = 0.032$ over the range $10^{-1.7} > t > 10^{-5.0}$ with reasonable coefficients. However, either correction would be consistent with a universal value of y in the range given by Eq. (43).

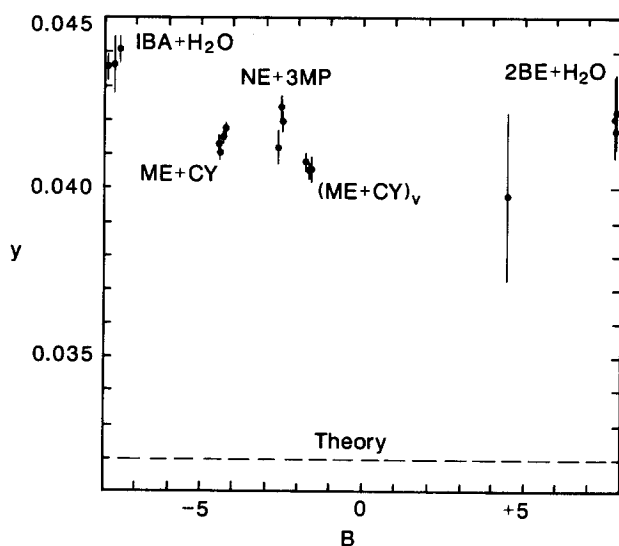


FIG. 7. The viscosity exponent y for 17 runs as a function of the background parameters B . [See Eq. (37).] All of the values lie considerably above 0.032, a recent theoretical result (Ref. 2). The error bars represent $\pm 1\sigma$ (68% confidence level). No significant sweep rate dependence was found. For example, sweep rates of the three NE + 3MP runs were 2, 9, and 39 $\mu\text{K/s}$ at T_c .

TABLE V. Comparisons at $t = 10^{-2}$ to other viscosity measurements.

Mixture	$\eta(\text{other})/\eta(\text{this work}) - 1$		
ME + CY	-0.5% (Ref. 17)	+0.7% (Ref. 16)	
IBA + H ₂ O	-2.5% (Ref. 30)	-2.2% (Ref. 31)	-0.1% (Ref. 32)
NE + 3MP	+4.1% (Ref. 33)	+0.7% (Ref. 34)	+2.6% (Ref. 35)
2BE + H ₂ O	+5.9% (Ref. 42)	-1.1% (Ref. 35)	+0.1% (Ref. 43)

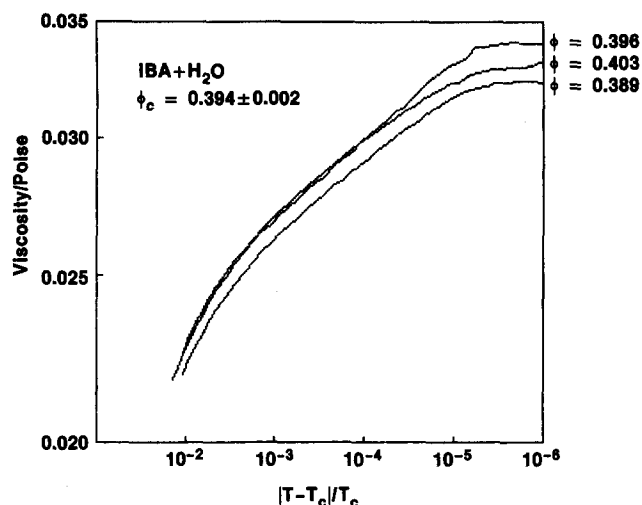


FIG. 8. Viscosity runs at three concentrations for isobutyric acid + water. The concentration nearest Φ_c shows the largest viscosity near T_c .

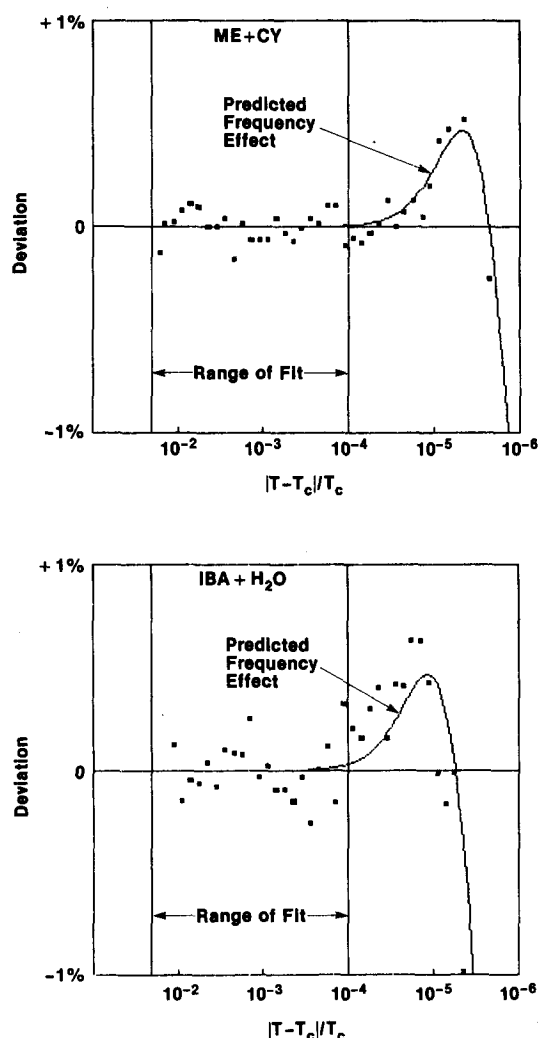


FIG. 9. Deviations from Eq. (37) ignoring the frequency effects of Eqs. (32) and (33), i.e., $F(\omega\tau) \equiv F(0) = 1$. The data show a 0.5% enhancement near $\omega\tau \approx 5$. The theory of Ref. 4 correctly predicts both the magnitude and location of this enhancement without adjustable parameters.

Because Eq. (37) describes the data extremely well with four parameters, additional free parameters can not extract more information from the experiments. Refinements of the theory of viscosity at moderate reduced temperatures which do not introduce additional free parameters would be useful. In its present form, the discrepancy between the theoretical and experimental values of the viscosity exponent γ cannot be explained.

C. Deviations from power-law behavior near the critical point

We encountered effects due to concentration errors and nonzero frequency. Figure 8 illustrates how concentration errors cause premature "rolloff" of the data close to T_c . As expected, the concentration closest to critical shows the largest viscosity enhancement.

As described in Sec. V B 3, we made use of an existing theory for frequency effects near T_c . Figure 9 shows the deviations which occur when the frequency effect is ignored. The enhancement of the effective viscosity at $\omega\tau \approx 5$ is a unique signature and is definitely visible. Similar enhancements were observed in the other two binary mixtures.

ACKNOWLEDGMENTS

J. G. Shanks loaded our spherical bob with the NE + 3MP mixture. We were also happy to receive useful advice from J. F. Douglas, R. A. Ferrell, R. W. Gammon, S. C. Greer, E. A. Kearsley, J. Kestin, G. Morrison, J. C. Nieuwoudt, G. A. Olchowy, and J. V. Sengers. This work has been supported in part by the Microgravity Sciences Program of NASA under Contract C-86129D.

- ¹J. V. Sengers, *Int. J. Thermophys.* **6**, 203 (1985).
- ²J. K. Bhattacharjee and R. A. Ferrell, *Phys. Rev. A* **28**, 2363 (1963).
- ³R. F. Berg and M. R. Moldover, *Int. J. Thermophys.* **7**, 675 (1986).
- ⁴J. K. Bhattacharjee and R. A. Ferrell, *Phys. Lett. A* **76**, 290 (1980); *Phys. Rev. A* **27**, 1544 (1983).
- ⁵D. W. Oxtoby, *J. Chem. Phys.* **62**, 1463 (1975).
- ⁶R. F. Berg and M. R. Moldover, *Rev. Sci. Instrum.* **57**, 1667 (1986).
- ⁷J. G. Shanks and J. V. Sengers (to be published); see Ref. 38.
- ⁸P. C. Hohenberg and B. I. Halperin, *Rev. Mod. Phys.* **49**, 435 (1977).
- ⁹T. Ohta, *J. Phys. C* **10**, 791 (1977); T. Ohta and K. Kawasaki, *Prog. Theor. Phys.* **55**, 1384 (1976).
- ¹⁰P. Debeye, B. Chu, and D. Woermann, *J. Polym. Sci. A* **1**, 249 (1963).
- ¹¹J. K. Bhattacharjee, R. A. Ferrell, R. S. Basu, and J. V. Sengers, *Phys. Rev. A* **24**, 1469 (1981).
- ¹²G. A. Olchowy and J. V. Sengers, Technical Report BN 1052 (1986), Institute for Physical Science and Technology, University of Maryland.
- ¹³H. L. Swinney and D. L. Henry, *Phys. Rev. A* **8**, 2586 (1973).
- ¹⁴J. V. Sengers, in *Transport Phenomena-1973*, edited by J. Kestin, AIP Conf. Proc. No. 11 (American Institute of Physics, New York, 1973), p. 229.
- ¹⁵J. Kestin and G. F. Newell, *Z. Angew. Math. Phys.* **8**, 433 (1957); D. A. Beckwith and G. F. Newell, *ibid.* **8**, 450 (1957).
- ¹⁶C. M. Sorensen, Ph.D. thesis, University of Colorado, Boulder, 1976.
- ¹⁷A. N. Campbell and S. C. Anand, *Can. J. Chem.* **50**, 1109 (1972), and associated unpublished data (deposit no. 248).
- ¹⁸N. V. Kuskova and E. V. Matizen, *Pis'ma Zh. Eksp. Teor. Fiz.* **12**, 255 (1970) [*JETP Lett.* **12**, 174 (1970)].
- ¹⁹S. Ballaró, G. Maisano, P. Migliardo, and F. Wanderlingh, *Phys. Rev. A* **6**, 1633 (1972).
- ²⁰Mallinkrodt, Inc., Paris, KY 40361, Spectr AR grade. In order to adequately describe materials and experimental equipment, we must occasionally state a manufacturer's name or label. This does not imply an endorsement by the National Bureau of Standards.

- ²¹J. L. Tveekrem and D. T. Jacobs, *Phys. Rev. A* **27**, 2773 (1983).
- ²²R. H. Cohn and D. T. Jacobs, *J. Chem. Phys.* **80**, 856 (1984).
- ²³C. Houessou, P. Guenoun, R. Gastaud, F. Perot, and D. Beysens, *Phys. Rev. A* **32**, 1818 (1985).
- ²⁴D. C. Jones and S. Amstell, *J. Chem. Soc.* **1930**, 1316.
- ²⁵E. L. Eckfeldt and W. W. Lucasse, *J. Phys. Chem.* **47**, 164 (1947).
- ²⁶R. R. Singh and W. A. Van Hook, *J. Chem. Phys.* **87**, 6097 (1987).
- ²⁷A. N. Campbell and E. M. Kartzmark, *Can. J. Chem.* **45**, 2433 (1967).
- ²⁸D. T. Jacobs, D. J. Anthony, R. C. Mockler, and W. J. O'Sullivan, *Chem. Phys.* **20**, 219 (1977).
- ²⁹R. B. Kopelman, R. W. Gammon, and M. R. Moldover, *Phys. Rev. A* **29**, 2048 (1984).
- ³⁰D. Woermann and W. Sarholz, *Ber. Bunsenges. Phys. Chem.* **69**, 319 (1965).
- ³¹J. C. Allegra, A. Stein, and G. F. Allen, *J. Chem. Phys.* **55**, 1716 (1971).
- ³²K. Hamano, S. Teshigawara, T. Koyama, and N. Kuwahara, *Phys. Rev. A* **33**, 485 (1986).
- ³³A. Stein, J. C. Allegra, and G. F. Allen, *J. Chem. Phys.* **55**, 4265 (1971).
- ³⁴B. C. Tsai and D. McIntyre, *J. Chem. Phys.* **60**, 1937 (1974).
- ³⁵I. L. Pegg and I. A. McLure, *Mol. Phys.* **53**, 897 (1984).
- ³⁶C. M. Sorensen, *Int. J. Thermophys.* **3**, 365 (1982).
- ³⁷H. C. Burstyn and J. V. Sengers, *Phys. Rev. A* **25**, 448 (1982).
- ³⁸J. G. Shanks, Ph.D. thesis, University of Maryland, 1986.
- ³⁹A. W. Wims, D. McIntyre, and F. Hynne, *J. Chem. Phys.* **50**, 616 (1969).
- ⁴⁰S. C. Greer and R. Hocken, *J. Chem. Phys.* **63**, 12 (1975).
- ⁴¹J. Reeder, T. E. Block, and C. M. Knobler, *J. Chem. Thermodyn.* **8**, 133 (1976).
- ⁴²Y. Izumi, A. Dondos, C. Picot, and H. Benoit, *J. Phys.* **42**, 353 (1981).
- ⁴³K. Hamano, T. Kawazura, T. Koyama, and N. Kuwahara, *J. Chem. Phys.* **82**, 2718 (1985).
- ⁴⁴Aldrich Chemical Co., Inc. Milwaukee, WI 53233, 99 + %, Spectrophotometric grade.
- ⁴⁵J. M. Grouvel and J. Kestin, *Appl. Sci. Res.* **34**, 427 (1978); W. Brockner, K. Torklepe, and H. A. Oye, *Ber. Bunsenges. Phys. Chem.* **83**, 1 (1979).
- ⁴⁶The four-parameter equation of J. F. Swindells, in *Handbook of Chemistry and Physics*, edited by R. C. West (Chemical Rubber, Cleveland, 1974) agrees within 0.1% over the range 20–60 °C with the recent representation of J. V. Sengers and B. Kamgar-Parsi, *J. Phys. Chem. Ref. Data* **13**, 185 (1984).
- ⁴⁷E. A. Kearsley, *Trans. Soc. Rheol.* **3**, 69 (1959).
- ⁴⁸J. T. Ho and J. D. Lister, *Phys. Rev. B* **2**, 4523 (1970); a concise summary of the restricted model is given in M. R. Moldover, J. V. Sengers, R. W. Gammon, and R. J. Hocken, *Rev. Mod. Phys.* **51**, 79 (1979).
- ⁴⁹A. Onuki and K. Kawasaki, *Phys. Lett. A* **75**, 485 (1980).
- ⁵⁰A. Onuki, Y. Yamazaki, and K. Kawasaki, *Ann. Phys.* **131**, 217 (1981).
- ⁵¹D. Beysens, M. Gbadamassi, and B. Moncef-Bonanz, *Phys. Rev. A* **28**, 2481 (1983).
- ⁵²H. C. Burstyn, J. V. Sengers, J. K. Bhattacharjee, and R. A. Ferrell, *Phys. Rev. A* **28**, 1567 (1983).
- ⁵³J. C. Nieuwoudt and J. V. Sengers, *Physica A* **147**, 368 (1987).
- ⁵⁴G. A. Olchowy and J. V. Sengers (private communication).
- ⁵⁵P. Calmettes, *Phys. Rev. Lett.* **39**, 1151 (1977).
- ⁵⁶S. C. Greer, *Phys. Rev. A* **14**, 1770 (1976).
- ⁵⁷W. V. Andrew, T. B. K. Khoo, and D. T. Jacobs, *J. Chem. Phys.* **85**, 3985 (1986).
- ⁵⁸D. T. Jacobs, *Phys. Rev. A* **33**, 2605 (1986).
- ⁵⁹D. Beysens, A. Bourgou, and P. Calmettes, *Phys. Rev. A* **26**, 3589 (1982).
- ⁶⁰See AIP document no. PAPS JCPA-89-3694-6 for 6 pages of averaged viscosity data. Order by PAPS number and journal reference from American Institute of Physics, Physics Auxiliary Publication Service, 335 East 45th Street, New York, NY 10017. The price is \$1.50 for each microfiche (98 pages) or \$5.00 for photocopies of up to 30 pages, and \$0.15 for each additional page over 30 pages. Airmail additional. Make checks payable to the American Institute of Physics.